Study of electron densities of methyl acetate, *N*-methylacetamide and *N*,*N*′-dimethylurea by quantum mechanical investigations. Part 2.[1] Solvent models

Bernd Kallies * and Rolf Mitzner

Institut für Physikalische und Theoretische Chemie, Universität Potsdam, 14469 Potsdam, Germany

The electron densities of a simple ester, amide and urea derivative have been studied with quantum mechanical methods at the Becke3LYP/6-31 + G* level. Solvent effects were modelled with an SCRF approach based on the SCI-PCM electrostatic continuum solvation model and with explicit inclusion of water molecules at different hydrogen bond donor–acceptor sites of the solutes. Discussions of electron densities use Natural Atomic (NAO) and Natural Bond Orbitals (NBO). Electrostatic interactions with a polar solvent yield polarization of the $\pi_{C=O}$ bond towards oxygen, a higher delocalization of lone pairs from –O– or –NH– into the $\pi^*_{C=O}$ anti-bond and a higher localization of lone-pairs at the carbonyl oxygen. Particular different changes in charge densities after explicit hydration of the molecules are discussed.

Introduction

Resonance and inductive substituent effects acting on the C=O group of carboxylic acid derivatives determine the behaviour of these compounds due to conformational changes and reactivity towards nucleophilic attack on the carbonyl carbon. It was shown by quantum mechanical calculations[1] on a structurally related ester, amide and urea in the gas phase, that the overall resonance stabilization increases in the series ester < amide < urea, although each nitrogen lone pair of urea is more localized than that of a similar amide. This result is associated with a barrier of rotation around one C(O)–NH bond in ureas that is of lower energy than that of related amides.

It is of major interest how the electron densities of these compounds, and thus their properties, are changed through external perturbations, *e.g.* through solvation by polar aprotic or protic solvents. It is well known that conformational equilibria and activation barriers strongly depend on the solubility of conformers and transition states.[2] Solvation of particular sites of a substrate by specific interactions with an enzymatic active site is a main source of enzymatic catalysis.[3]

In order to give an insight into the behaviour of charge distributions of a structurally related ester, amide and urea after overall and particular solvation, the present study was undertaken.

Computational details

The calculations were carried out with the GAUSSIAN94/DFT package[4] on IBM RS/6000 workstations at the University of Potsdam and on a CRAY Y-MP4E/464 at the Konrad-Zuse-Zentrum für Informationstechnik Berlin (ZIB). The results were produced using density functional theory (DFT) at the Becke3LYP/6-31 + G* level[5,6] as described previously.[1]

We estimated the effects of solvation by a polar solvent by a Self Consistent Reaction Field (SCRF) approach. Therefore we chose the Self Consistent Isodensity Polarized Continuum Model (SCI-PCM)[7] using a relative permittivity of 78.5. PCM models[8] use apparent solvent charges resting on the surface of the solute to give access to the electrostatic part of the solvation free energy (electrostatic interactions between the solute and an external electric field, solvent polarization). I-PCM models define the cavity of the solute by its electron density through an isodensity level, rather than using regular bodies or combinations of them. We used an isodensity level of 0.0004 au, since it seems to be a good choice to represent experimentally measured liquid molar volumes.[9] The SCI-PCM model determines the quantum description of the solute (wavefunction or electron density), the shape of the cavity and the solvent charge distribution in a self consistent manner rather than using an unperturbed gas phase cavity. Self consistency is determined by convergence of the wavefunction and not by convergence of solvent charges.

Studies of solvent effects on conformations used the gas phase optimized B3LYP/6-31 + G* geometries and gas phase partition functions of the solutes. Assuming that geometry changes and changes of partition functions are small when going from the gas phase to a solvated state, the calculated difference between energies of a solute with and without the used solvent model corresponds to the electrostatic part of the solvation free energy. The remaining contributions to the solvation free energy (cavitation energy, contributions from other intermolecular interactions like hydrogen bonds or dispersion interactions) were not considered in this paper.

For discussions of electron densities the geometries were further optimized with inclusion of solvent effects. In order to describe changes in electron densities arising from hydrogen bonds we included explicit water molecules at different sites of the solutes in their preferred ground state conformations. The aggregates were fully optimized at the B3LYP/6-31 + G* level using appropriate symmetry constraints. The usefulness of modern DFT techniques in order to obtain geometries and interaction energies of various types of weak interacting systems has been shown recently.[10] Association energies were calculated as the difference between the energy of the complex and the energies of the isolated monomers. Force constant calculations were not performed. The basis set superposition error (BSSE) of the interaction energy was estimated by the counterpoise procedure[11] for the complexes with one water molecule.

Discussions of charge distributions are based upon analyses of Natural Atomic Orbitals (NAO) and Natural Bond Orbitals (NBO),[12–14] as implemented in the NBO 3.0 program.[15]

Results and discussion

Conformational analyses

The studied conformers of methyl acetate (MAC), *N*-methylacetamide (MAM) and *N*,*N*′-dimethylurea (DMU)

Table 1 Enthalpies of activation and reaction, gas phase dipole moments and solvation energies[a]

Preferred conformation	ΔH(298 K)[b]/kcal mol^{-1} SCI-PCM	(Gas phase)	μ/D	ΔE_{Solv}[c]/ kcal mol^{-1}
MAC I			1.960	−3.61
MAM I			4.070	−6.70
DMU I *R,R*			3.867	−6.90
Other conformations				
MAC II	4.43	(7.65)	4.825	−6.84
MAM II	2.91	(2.22)	4.369	−6.01
DMU I *R,S*	−0.21	(0.63)	4.256	−7.74
DMU II *R,S*	0.18	(0.83)	4.358	−7.55
DMU III *R,R*	4.69	(5.10)	4.168	−7.31
Transition states of rotation and inversion				
MAC TS	11.15	(12.50)	3.555	−4.96
MAM TS1	19.99	(17.52)	1.815	−4.23
MAM TS2	21.07	(21.06)	4.098	−6.69
DMU TS1	8.61	(7.56)	2.771	−5.85
DMU TSi	−0.71	(0.04)	4.244	−7.65

[a] The conversion factor 1 au = 627.5095 kcal mol^{-1} was used; 1 cal = 4.184 J. [b] Enthalpy differences use the preferred conformation as reference. ΔH(SCI-PCM) is calculated from ΔH(Gas phase), adding the difference in solvation energies. [c] Difference between total energies from SCI-PCM calculations and gas phase energies using gas phase optimized geometries. The reported quantity is an approximation of the electrostatic component of the solvation free energy of a compound.

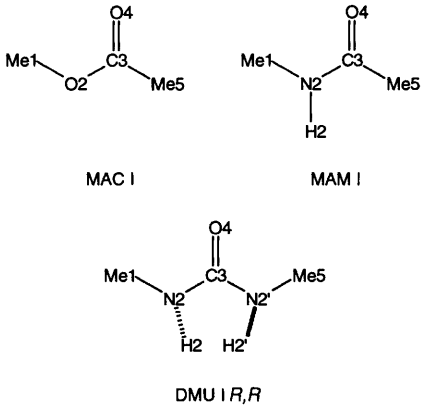

consist of rotamers around the –C(O)–X bonds and of stereoisomers related to inversion of the pyramidal NH centres of DMU. The structures which exhibit the common *trans* conformation with θ(C1–X2–C3–C5), θ(C1–X2–C3–X2′) and θ(X2–C3–X2′–C5) near 180° (conformers I) are found to be the preferred gas phase conformation for all the molecules studied.[1] The enthalpies of activation and reaction for going from conformer I to the transition states or other conformers are summarized in Table 1. The estimation of electrostatic effects of a polar (aprotic) solvent on the conformations does not alter the gas phase behaviour in general, except for the preferred stereoisomer of DMU. This would be expected for any reaction where only uncharged species are involved. Stabilizing or destabilizing effects of a polar solvent on the activation parameters of conformational changes can be attributed to changes in the dipole moments.[16] The calculated dipole moments of stationary points in the gas phase agree well with the observed effect of a solvent on rotational barriers and reaction enthalpies (see Table 1). The exception is the reaction MAM I→MAM II. The solvation energy of MAM II is calculated to be lower than that of MAM I, although its gas phase dipole moment is increased. The solvation of MAC yields a lower rotational barrier than in the gas phase, because its dipole moment rises upon rotation. Interestingly, the DMU I

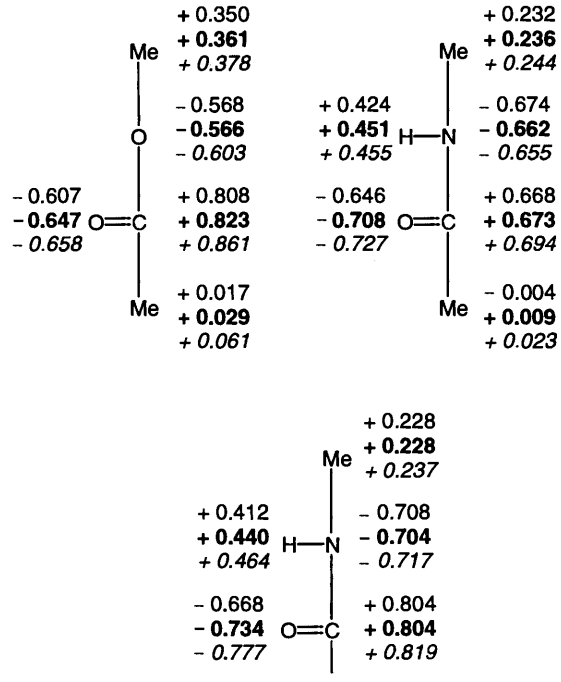

Fig. 1 Net atomic and group charges of MAC, MAM and DMU (gas phase: first value, SCI-PCM: bold typed, clusters shown in Fig. 2: italic typed). DMU exhibits a two-fold symmetry axis including the C=O bond, so only one half of the molecule is shown.

R,S conformation seems to become the preferred stereoisomer in solution. However, this result might be produced by the use of gas phase geometries. The increase in rotational barriers on solvation of secondary amides has been reported recently;[17] the description of effects of aprotic solvents with increasing polarity on rotational barriers of *N,N*-dimethyl-formamide and -acetamide by an isodensity polarized continuum model was demonstrated to be in surprising agreement with experimental data, presupposing a high level of theory and appropriate thermal corrections. It was also shown in this report, that the reduction of solvent–solute interactions to their electrostatic components is less accurate, if the effects of protic solvents like water have to be modelled. This apparent discrepancy can be discussed in detail by studying electron densities of organic molecules in the gas phase and with different solvation models. The calculations we present in the following sections deal with the ability of quantum mechanical methods to describe some fundamental sources of solvent effects on measurable phenomena.

Charge distributions

Electrostatic continuum solvation models are able to describe effects from interactions between permanent and induced multipoles. These interactions make the main contribution to the solvation energy of polar solutes in polar solvents.[2] It was shown in ref. 18 using an SCRF approach on sulfamic acid that solvation with a polar solvent allows solute residues with a partial excess of electrons to gain additional electron density. The net charges shown in Fig. 1 indicate a similar behaviour of simple carboxylic acid derivatives. The use of Mulliken population analyses instead of populations of NAOs yields similar general behaviour except for charges at the X2 atoms. Mulliken charges of these atoms become more negative after solvation.

In order to describe the polarizing effects of interactions with polar solvents in detail, population analyses of NBOs were undertaken. For a detailed description of this method see ref. 14. The transformation of the NAO basis set into NBOs yields the assumed Lewis structure of carboxylic acid derivatives which includes σ_{C3-O4}, $\pi_{C3=O4}$, σ_{X2-C3} bonds and corresponding

Table 2 Selected geometries and results from NBO analyses

	Gas phase			SCI-PCM		
Geometries	MAC	MAM	DMU	MAC	MAM	DMU
r(C3=O4)/Å	1.214	1.229	1.229	1.220	1.240	1.241
r(C3–X2)/Å	1.354	1.365	1.386	1.348	1.355	1.376
r(N2–H2)/Å		1.009	1.013		1.011	1.012
θ(H2–N2–C3–O4)/degrees		180.0	−155.8		180.0	−164.4
Percentage of total electron density in Lewis structures	98.658	98.540	98.465	98.657	98.495	98.405
Occupancies of NBOs/electrons						
LP X2	3.760[a]	1.709	1.788[b]	3.753[a]	1.680	1.764[b]
LP O4[c]	3.828	3.846	3.832	3.838	3.861	3.847
$\pi^*_{C3=O4}$	0.221	0.295	0.373	0.232	0.328	0.421
σ^*_{C3-X2}	0.106	0.075	0.075[b]	0.101	0.069	0.069[b]
σ^*_{C3-C5}	0.052	0.056		0.049	0.051	
Polarization coefficients (%) of NHOs in two-centre NBOs						
O4 (sp^2 in $\pi_{C3=O4}$)	69.91	71.18	72.57	71.23	73.10	74.82
X2 (sp^3 in σ_{C3-X2})	69.29	62.73	61.70	69.26	62.46	61.51
X2 (sp^3 in σ_{X2-H2})		71.58	71.00		72.90	72.32

[a] O2 of MAC contains two lone pairs, N2 of MAM and DMU only one. [b] Only one nitrogen centre counted. [c] Sum over occupancies of the two lone pairs at O4.

anti-bonds, two lone pairs at O4 and O2, and one lone pair at N2 and N2′. We use occupancies of the most important NBOs (see Table 2). In order to describe solvent effects on bond orbital polarization we also report polarization coefficients of two-centre-bonds which were normalized to give a sum of 100%.† In comparison with gas phase calculations, electrostatic solvent effects yield polarization mainly of the $\pi_{C3=O4}$ bond orbitals. Considering the occupancies of NBOs (see Table 2), we find additional electron density in the lone pairs of the carbonyl oxygen and in the $\pi^*_{C3=O4}$ anti-bonds. This behaviour is associated with higher delocalization of the X2 lone pair(s) into the $\pi^*_{C3=O4}$ anti-bond and higher localization of the carbonyl oxygen lone pairs, which are delocalized by a small amount into the σ^*_{C3-X2} anti-bond. These results are underlined by geometry changes upon solvation (see Table 2). The lengths of the C3–X2 bonds decrease, whereas the C3=O4 bonds are elongated. The nitrogen centres of DMU become more planar. The net effect of changes in electron delocalization is an increasing overall resonance. It can be roughly estimated by the sum of electrons found in the core and bonding NBOs and lone pairs, which amounts to about 98% of the total electron density (see Table 2). After inclusion of solvent effects it is further decreased.

These results can be explained by drawing alternative Lewis structures which describe electron delocalization in carboxylic acid derivatives (see Fig. 2). The changes in geometries, atomic charges and occupancies of NBOs we reported are consistent with the assumption of increasing weights of the structures II and III, leading to an increased overall resonance stabilization and C=O bond polarization by solvation by a polar solvent. That is the same as considering the zwitterionic structures II and III to exhibit a higher solubility than the neutral structure I.

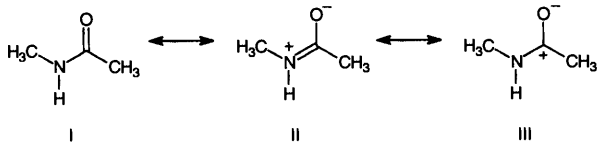

I II III

Fig. 2 Alternative Lewis structures for a carboxylic acid amide

Effects of hydrogen bonding

The hydrogen bonded clusters studied are explained in Fig. 3 and Table 3. The cartesian coordinates of all complexes are given as supplementary material.‡ The aggregates with maximal occupancy of all hydrogen bond acceptor and donor sites of the solutes should be discussed briefly by atomic charges only (see Fig. 1). The overall effect of inclusion of specific interactions between a solute and water molecules does not change the charge distributions qualitatively in our series compared with SCI-PCM results. The effects on electron densities discussed in the previous section are increased in their magnitude. This finding is not surprising since electrostatic forces are the main contribution to the interaction energy in neutral hydrogen bonded systems.[19] The remaining part of specific interactions between protic solvents and a solute includes charge transfer coupled with the formation of hydrogen bonds. It may be discussed mainly in strong interacting charged hydrogen bonded clusters.[20] Nevertheless, the study of partial hydrated solutes provides insight into details of the charge transfer process. The following discussions will be focused on this intention.

The association energies calculated for partial hydrated solutes are summarized in Table 3. The hydrogen bond lengths are not given, because they are strictly correlated with the association energy. The clusters presented there were fully optimized again, except DMU-b and DMU-c (see below). The positions of water molecules in complexes DMU-a differ from those shown in Fig. 3. In partial hydrated complexes they are located near the molecule plane as in complexes of MAC and MAM. This position is the one expected from the locations of the lone pairs at O4. The location of water molecules at the carbonyl oxygen perpendicular to the plane shown in Fig. 3 is caused by interactions between all water molecules, which form a hydrogen bonded solvation shell. The formation of this

† A σ_{AB} bonding orbital and its corresponding σ^*_{AB} anti-bond are formed from two hybrid orbitals h_A and h_B by linear combination: $\sigma_{AB} = c_A h_A + c_B h_B$, $\sigma^*_{AB} = c_A h_A - c_B h_B$. The coefficients c_A and c_B show the percentage of the σ_{AB} orbital on the two hybrids. They can be interpreted in terms of bond orbital polarization. We call them polarization coefficients.

‡ Suppl. Pub. 57146 (5 pp.). For details of the British Library Supplementary Publications Scheme, see 'Instructions for Authors (1996)', *J. Chem. Soc., Perkin Trans. 2*, 1996 issue 1.

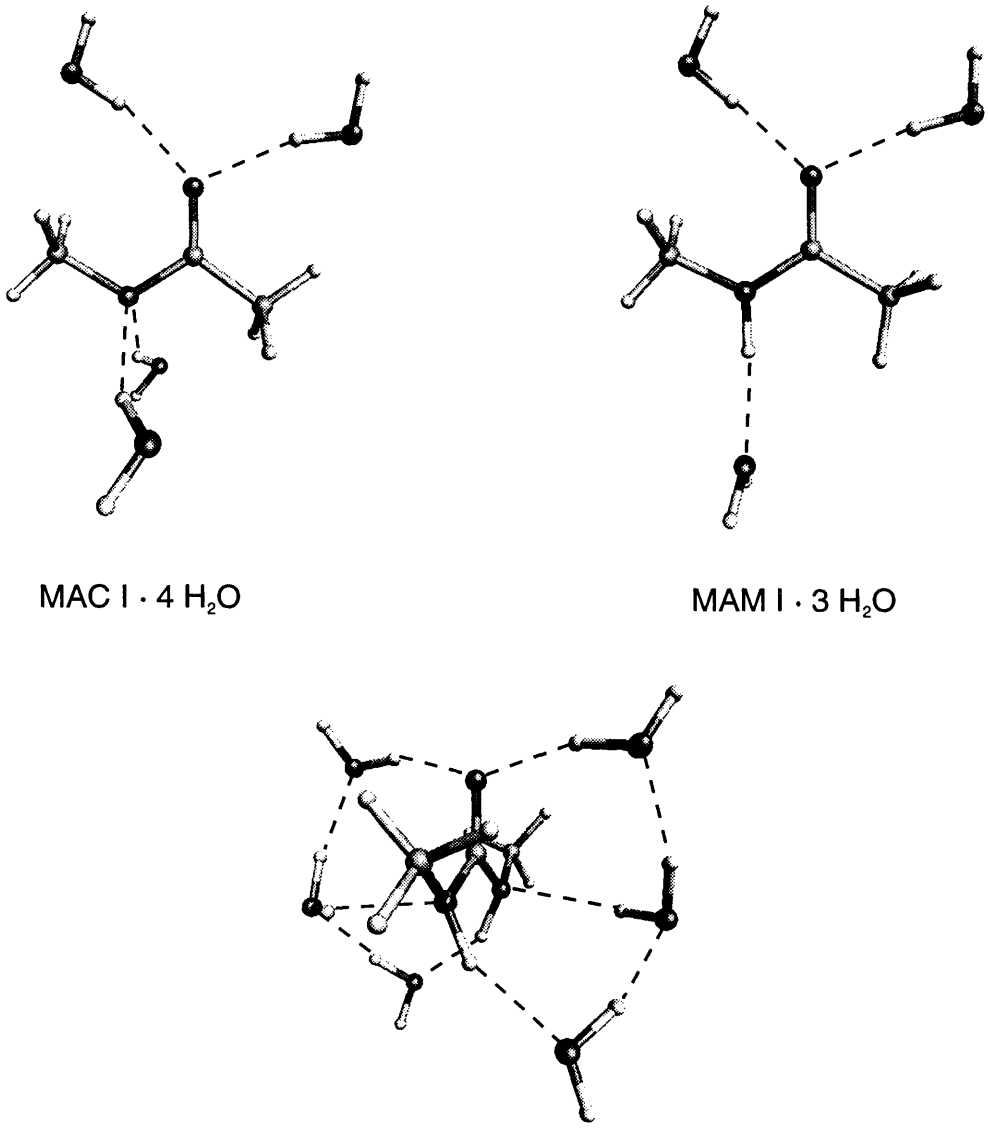

Fig. 3 Models with maximal possible occupancies of hydrogen bond donor–acceptor sites with water molecules. Dashed lines represent hydrogen bonds.

hydrogen bonded network seems to be preferred over the situation where the solvent molecules occupy the correct positions for interactions with lone pairs.

Our estimation of BSSE yields a decrease in the amounts of association energies for models with one water molecule by about 0.5–1 kcal mol^{-1}.§ Although BSSE makes about 10–15% of the association energies, it does not alter the relative strength of interaction in the series described here. So we did not include this correction in the table, but it still provides a good criterion for the usefulness of the chosen level of theory.[21] Table 3 contains additional information about the charge transfer process. We again use charges from NAOs and occupancies of NBOs and compare them with results from gas phase calculations. The use of populations of NAOs is strongly recommended here, since net atomic charges from Mulliken population analyses often yield a net charge transfer in the false direction if the monomers interact through weak but highly polar covalent bonds.[20]

§ 1 cal = 4.184 J.

The association energies of single solvated molecules indicate the carbonyl oxygen of all compounds to be the preferred site of hydrogen bonding. This result agrees with the fact that this atom is the preferred site of protonation in acyl derivatives.[22] It permits comparison in our series. The rising delocalization of the X2 lone pairs into the $\pi^*_{C=O}$ anti-bonds coupled with shortening of the C3–X2 bond and polarization of the $\pi_{C=O}$ bond toward oxygen is the main change in charge distribution compared with the isolated molecules in the gas phase. It was the main solvent effect obtained with SCI-PCM, too. Differences in charge densities calculated with the two solvation models arise mainly from the transfer of electron density from a hydrogen bond acceptor site onto the donor molecule which cannot be described by the SCI-PCM model. In our series, the lone pairs at the carbonyl oxygen are the sites mainly influenced by hydrogen bonding. SCI-PCM calculations yielded a higher localization of these electrons than in the gas phase (see Table 2), whereas explicit hydration yields a higher delocalization of them (see Table 3). It was shown by NBO analyses of various small hydrogen bonded compexes[14] that the transfer of electron density from a hydrogen bond acceptor site B onto a H

Table 3 Partial hydrated complexes: association energies and description of charge transfer

Complex[a]	ΔE_{Ass}[c]/kcal mol^{-1}	ct[d]	Change of occupancies of NBOs[b] $\Sigma\sigma^*_{A-H}$[e]	LP O4	$\Sigma\sigma^*_{C3-N2}$[f]	LP X2[f]	$\pi^*_{C3=O4}$
1 H_2O at O4							
MAC-a1	−6.51	−0.020	+0.024	−0.006	−0.009	−0.010	+0.015
MAM-a1	−8.01	−0.030	+0.032	−0.013	−0.007	−0.015	+0.021
DMU-a1	−7.71	−0.022	+0.026	−0.008	−0.013	−0.029	+0.032
2 H_2O at O4							
MAC-a2	−11.87	−0.032	+0.046	−0.008	−0.012	−0.026	+0.034
MAM-a2	−14.84	−0.048	+0.054	−0.021	−0.012	−0.035	+0.048
DMU-a2	−14.84	−0.042	+0.052	−0.009	−0.024	−0.067	+0.074
H_2O at X2 (X2: H-Bond acceptor)							
MAC-b1	−3.90	−0.014	+0.018	−0.005	+0.008	+0.004	−0.014
MAC-b2	−6.36	−0.022	+0.032	−0.011	+0.048	+0.015	−0.031
DMU-b2[g]	−9.47	−0.058	+0.065	−0.002	+0.005	±0.000	−0.048
H_2O at H2 (X2–H2: H-Bond donor)							
MAM-c1	−5.51	+0.017	+0.015	+0.024	−0.002	−0.015	+0.012
DMU-c2[g]	−7.44	+0.044	+0.042	+0.003	±0.000	+0.014	−0.015

[a] Complexes a: hydration of the carbonyl oxygen; complexes b: hydration of lonepairs at X2; complexes c: hydration of the H2 sites. The number represents the water molecules added to a solute. [b] Compare with occupancies in isolated molecules in the gas phase, see Table 2. [c] Uncorrected difference between the total energies of the complex and the isolated monomers in the gas phase. [d] Overall charge transfer in electrons. Negative signs indicate electron loss of the solute. [e] A–H is the hydrogen bond donor group: O–H in the case of water (complexes a and b), N–H in the case of complexes c. [f] NBOs including N2 and N2′ of DMU added up. [g] NH groups occupied by one water molecule each.

bond donor site AH through formation of an A–H···B aggregate is visualized by the delocalization of lone pair electrons from B into the σ^*_{A-H} anti-bond using the NBO picture. We again observe this behaviour (see Table 3). (From the viewpoint of overall electron density charge transfer is visible in the formation of a weak covalent bond between H and B and in the polarization of the A–H bond toward A. NBO calculations omit the bond orbital for the H···B bond because it would be associated with a change in the Lewis structure.) The amount of additional electron density found in the σ^*_{A-H} anti-bonds follows the same order as the calculated overall charge transfer and the association energies for these complexes, which rise in the series MAC < DMU < MAM. If one looks at partial charges of the carbonyl oxygens in the gas phase (see Fig. 1), a slightly different order of hydrogen bond strength would be assumed. The high amount of electron density found at O4 in DMU should yield the strongest hydrogen bond in the series. If one remembers that the molecular background of the atoms participating in a hydrogen bond is involved in the charge transfer process depending on the polarizability of its electron density, then again DMU should show the highest association energy. But our results indicate DMU to be a poorer hydrogen bond acceptor at O4 than MAM. The discrepancy between the assumed and calculated behaviour of DMU is difficult to separate because the net association energy of hydrogen bonded clusters is influenced by at least four components: (*a*) the ability of the H-bond acceptor to donate electrons (*b*) the ability of the H-bond donor to accept additional charge, (*c*) other components of the interaction energy like electrostatic and dispersion contributions and (*d*) the energy required for deformation of the monomers when they approach each other. From this point of view two explanations would be possible for the unusually low association energies of the complexes DMU-a1 and DMU-a2. The first states simple steric hindrance between the methyl groups of DMU in the studied *trans–trans* conformation and the water molecules at O4. The second uses the amount of delocalization of lone pair electrons from O4 into other bonds. The occupancies of the carbonyl oxygen lone pairs in the isolated molecules (see Table 3) show the same order as found for association energies. The amount of delocalization of these electrons into the σ^*_{C3-N2} and σ^*_{C3-C4} anti-bonds seems to represent a measure of the possibility of their delocalization toward a hydrogen bond donor.

The electron flux in the solutes after explicit hydration of other sites will be discussed briefly in the following section. MAC presents a second hydrogen bond acceptor site at its ether oxygen. As assumed from association energies (see Table 3), the amount of charge transfer into the water molecule(s) is lower than that stated for hydration of the carbonyl oxygen. The main change in electron density is a lowering of delocalization of the lone pair electrons at O2 into the $\pi^*_{C=O}$ bond compared with gas phase calculations. On the other hand lone pair electrons from O4 become a bit more delocalized. The overall effect on geometry is a lengthening of the C3–O2 bond by about 0.01 Å, but only a slight shortening of the C3=O4 bond by about 0.005 Å.

The NH group of MAM serves as a hydrogen bond donor site. After single hydration the solute gains 0.017 electrons from the water molecule, but this additional electron density does not lie at the nitrogen atom. We find it mainly in the lone pairs of the carbonyl oxygen and to a lesser extent in the $\pi^*_{C=O}$ anti-bond. We state that only slight geometry changes occur compared with the gas phase, but the negative charge at the carbonyl oxygen rises by 0.014 electrons! This finding agrees well with the high amount of resonance stabilization of this molecule which makes transport of electron density over wide distances onto the most electronegative site possible.

Our intention to study the single hydration of only one NH group of DMU by full geometry optimization failed. Geometry optimizations with one water molecule led to association of both NH hydrogens with the water oxygen. Structures with two water molecules led to a symmetric aggregate which exhibits formation of a hydrogen bond between a water oxygen and the NH hydrogen of N2, and a H-bond between a hydrogen of the same water molecule and the nitrogen lone pair of N2′. This structure shows a change in electron distribution which is hard to divide into components, because each NH group serves both as electron donor and acceptor. In order to separate effects from hydrogen bond formation at the NH hydrogens and the N lone pairs we built an aggregate of DMU with four water molecules (see Fig. 3 without hydration of the carbonyl oxygen). From the structure obtained two water molecules were deleted in each case to give hydration of the desired sites. Here only single point calculations were performed, so the results

presented in Table 3 can only give a rough estimation of the behaviour of the systems. Hydration of the nitrogen lone pairs (DMU-b2) seems to be preferred over hydration of the NH hydrogens (DMU-c2). The latter complex may be compared with MAM-c1. As assumed by the difference in lone pair delocalization at one nitrogen in MAM and DMU, the charge introduced by the water molecules stays at the nitrogens of DMU and is not transferred onto the carbonyl oxygen as in MAM-c1. This behaviour causes a reduction in the resonance stabilization of DMU, whereas it was increased in the case of MAM. Complex DMU-b2 may be compared with MAC-b1/b2. The qualitative behaviour of these systems is similar. The electron density associated with delocalization of the X2 lone pairs into the $\pi^*_{C3=O4}$ anti-bond in the isolated molecule is used for formation of hydrogen bonds in the complex.

Acknowledgements

This work was funded by the Deutsche Forschungsgemeinschaft, DFG-Gz.INK 16/A1-1. We thank Dr Steinke for his kind assistance in using the resources at ZIB.

References

1 B. Kallies and R. Mitzner, *J. Chem. Soc., Perkin Trans. 2*, 1996, preceding paper.
2 C. Reichardt, *Solvent effects in organic chemistry*, VCH, Weinheim, Basel, Cambridge, New York, 1978.
3 A. Warshel, *Computer modeling of chemical reactions in enzymes and solutions*, Wiley, New York, 1991.
4 GAUSSIAN94, Revision B.1, M. J. Frisch, G. W. Trucks, H. B. Schlegel, P. M. W. Gill, B. G. Johnson, M. A. Robb, J. R. Cheeseman, T. A. Keith, G. A. Petersson, J. A. Montgomery, K. Raghavachari, M. A. Al-Laham, V. G. Zakrzewski, J. V. Ortiz, J. B. Foresman, J. Cioslowski, B. B. Stefanov, A. Nanayakkara, M. Challacombe, C. Y. Peng, P. Y. Ayala, W. Chen, M. W. Wong, J. L. Andres, E. S. Replogle, R. Gomperts, R. L. Martin, D. J. Fox, J. S. Binkley, D. J. Defrees, J. Baker, J. J. P. Stewart, M. Head-Gordon, C. Gonzalez and J. A. Pople, Gaussian, Inc., Pittsburgh PA, 1995.
5 P. C. Hariharan and J. A. Pople, *Theor. Chim. Acta*, 1973, **28**, 213.
6 A. D. Becke, *J. Chem. Phys.*, 1993, **98**, 5648.
7 T. A. Keith and M. J. Frisch, submitted for publication.
8 J. Tomasi and M. Persico, *Chem. Rev.*, 1994, **94**, 2027.
9 K. B. Wiberg, H. Castejon and T. A. Keith, *J. Comput. Chem.*, 1996, **17**, 185.
10 P. Hobza, J. Sponer and T. Reschel, *J. Comput. Chem.*, 1995, **16**, 1315.
11 S. F. Boys and F. Bernardi, *J. Mol. Phys.*, 1970, **19**, 553.
12 A. E. Reed, R. B. Weinstock and F. Weinhold, *J. Chem. Phys.*, 1985, **83**, 735.
13 J. P. Foster and F. Weinhold, *J. Am. Chem. Soc.*, 1980, **102**, 7211.
14 A. E. Reed, L. A. Curtiss and F. Weinhold, *Chem. Rev.*, 1988, **88**, 899.
15 A. E. Reed and F. Weinhold, *QCPE Bull.*, 1985, **5**, 141.
16 T. Drakenberg, K. J. Dahlqvist and S. Forsen, *J. Phys. Chem.*, 1972, **76**, 2178.
17 K. B. Wiberg, P. R. Rablen, D. J. Rush and T. A. Keith, *J. Am. Chem. Soc.*, 1995, **117**, 4261.
18 M. W. Wong, K. B. Wiberg and M. J. Frisch, *J. Am. Chem. Soc.*, 1992, **114**, 523.
19 S. Scheiner, in *Reviews in Computational Chemistry II*, eds. K. B. Lipkowitz and D. B. Boyd, VCH, New York, Weinheim, Cambridge, 1991, p. 165.
20 B. Kallies and R. Mitzner, *J. Mol. Model.*, 1995, **1**, 68.
21 F. B. van Duijneveldt, J. G. C. M. van Duijneveldt-van de Rijdt and J. H. van Lenthe, *Chem. Rev.*, 1994, **94**, 1873.
22 R. I. Zalewski, in *The Chemistry of Functional Groups*, ed. S. Patai, Wiley, Chichester, 1992, suppl. B, vol. 2, part 1, p. 305.

Paper 5/08363J
Received 28*th December* 1995
Accepted 19*th March* 1996